

# Bernoulli potential in type-I and weak type-II superconductors: III. Electrostatic potential above the vortex lattice

Pavel Lipavský<sup>1,2</sup>, Klaus Morawetz<sup>3,4</sup>, Jan Koláček<sup>2</sup>, Jiří J. Mareš<sup>2</sup>, Ernst Helmut Brandt<sup>5</sup> and Michael Schreiber<sup>3</sup>

<sup>1</sup>*Faculty of Mathematics and Physics, Charles University, Ke Karlovu 5, 121 16, Prague 2, Czech Republic*

<sup>2</sup>*Institute of Physics, Academy of Sciences, Cukrovarnická 10, 16253 Prague 6, Czech Republic*

<sup>3</sup>*Institute of Physics, Chemnitz University of Technology, 09107 Chemnitz*

<sup>4</sup>*Max-Planck-Institute for the Physics of Complex Systems, Noethnitzer Str. 38, 01187 Dresden, Germany*

<sup>5</sup>*Max-Planck-Institute for Metal Research, D-70506 Stuttgart, Germany*

The electrostatic potential above the Abrikosov vortex lattice, discussed earlier by Blatter *et al.* [PRL **77**, 566 (1996)], is evaluated within the Ginzburg-Landau theory. Unlike previous studies we include the surface dipole. Close to the critical temperature, the surface dipole reduces the electrostatic potential to values below sensitivity of recent sensors. At low temperatures the surface dipole is less effective and the electrostatic potential remains observable as predicted earlier.

## I. INTRODUCTION

A boundary between the normal and superconducting states is characterized by two length scales. First, the local fraction of superconducting electrons is measured by the Ginzburg-Landau (GL) wave function  $\psi$  which changes on the scale of the GL coherence length  $\xi$ . Second, there is a magnetic field  $\mathbf{B}$  screened on the scale of the London penetration depth  $\lambda$ . This picture is common to type-I superconductors, in which the superconducting state is nearly separated from the normal state, and to type-II superconductors, in which the normal state is dispersed into individual lines called vortices.

In extreme type-II superconductors, where  $\xi \ll \lambda$ , the spatial shape of the superconducting fraction provides a sharper image of vortices than the spatial dependence of the magnetic field. Blatter *et al.*<sup>1</sup> proposed to observe the space modulation of the superconducting fraction via the electrostatic field that is expected to develop above a surface of superconductors. Their estimate of the electric field created by the Abrikosov vortex lattice predicts values well observable by recent experimental tools.

The idea of Blatter *et al.* is as follows. According to theoretical predictions,<sup>2–4</sup> the space modulation of the superconducting gap  $\Delta$  induces a charge transfer so that an electrostatic potential (called the Bernoulli potential) develops inside the superconductor. Since the Bernoulli potential  $\phi$  is a function of the square of the gap,  $\phi$  can be used to observe  $|\Delta|^2$ . The GL wave function is linearly proportional to the superconducting gap, i.e.,  $\phi$  can be used to observe  $|\psi|^2$ .

The Bernoulli potential cannot be detected inside the superconductor, it leaks out from the surface, however. Its detection outside might be possible by scanning force microscopy or using the Kelvin capacitive pickup with a single-electron transistor as a sensor.<sup>1</sup>

As far as we know, such an experiment has not been performed yet, but it is under preparation. It is likely

that the experimental setup will first be tested on conventional superconductors.<sup>5</sup> In this paper we show that close to the critical temperature the electrostatic potential above the surface is strongly reduced by the surface dipole, which arises due to unbalanced pairing forces.<sup>6</sup> At lower temperatures the surface dipole is not so effective and the electrostatic field reaches observable amplitudes.

The paper is organized as follows. In the next section we specify the assumed experimental situation and the physical picture of charge transfer contributing to the expected electrostatic potential. In Sec. III we derive a relation between the GL wave function and the electrostatic potential and provide a simple estimate of the potential for the magnetic field far from the upper critical field, i.e., for the limit of separated vortices. In Sec. IV we discuss numerical results, and in Sec. V we summarize.

## II. BASIC ASSUMPTIONS

Let us first describe the experimental situation we assume in our discussion. A superconducting film fills the layer  $-L < z < 0$ . This film is thin on the characteristic scales of the GL theory,  $L \ll \xi, \lambda$ , but it is thick with respect to the BCS coherence length,  $L \gg \xi_0$ . The magnetic field  $\mathbf{B}||z$  penetrates the superconductor in form of vortices. The electrostatic potential will be scanned close to the surface at  $z_{\text{scan}} > 0$ .

Now we turn to the underlying physical picture. The electrostatic potential leaking out of the superconductor is generated by charges that can be sorted into three groups: **A.** the bulk charge, **B.** the surface dipole, and **C.** the surface charge. These contributions are discussed in individual subsections.

### A. Bulk charge

The bulk charge covers a transfer of electrons from the inner to the outer regions of the vortices. There are various forces taking part in this transfer. First, electrons rotate around the vortex center so that the inertial force acts in the centrifugal direction. Second, the magnetic field pushes electrons via the Lorentz force – also pointing outward. Third, the energy of Cooper pairs is lower than the energy of free electrons, therefore unpaired electrons in the vortex core are attracted towards the condensate around the core. The resulting force again points outward. These forces deplete the electron density in the vortex core, creating the Coulomb force which balances all the other forces.

Due to these various contributing mechanisms, there is no single characteristic length scale of the charge modulation. The shortest scale is the GL coherence length  $\xi$  reflecting the pairing forces. The contribution of the inertial and the Lorentz forces change on the scale of the London penetration depth  $\lambda$ . The long-range periodicity is of course enforced by the Abrikosov vortex lattice.

The bulk charge has been evaluated within various approximations mostly covering only some of the acting forces. Studies based exclusively on the Lorentz and the inertial forces have been performed within the classical picture of the superconducting fluid<sup>7</sup> and later with its quantum form.<sup>8</sup>

In the last decade, the charge transfer in vortices has been derived from the electron-hole non-symmetry of the density of states at the Fermi level.<sup>3,4</sup> Later it was recognized that the electron-hole non-symmetry effects are identical to forces due to the pairing energy.<sup>9,10</sup> In result there are two scientific dialects for the pairing forces. We prefer the original one.

Approaches that cover all the above listed forces are either phenomenological or microscopic. The phenomenological studies<sup>11</sup> use the theory of the GL type. The microscopic studies<sup>12–16</sup> are based on the Bogoliubov-de Gennes theory. It is worth to mention that in the vicinity of  $T_c$  the electrostatic potential obtained from the microscopic studies agrees with the result of the GL theory.<sup>12–16</sup>

The microscopic theory is superior to the others as it covers all important contributing mechanism in a unified way<sup>16</sup> and its region of applicability is not restricted to the vicinity of  $T_c$  or to small gradients of the superconducting gap. On the other hand, such complete treatment is complicated and numerically demanding. Here we use the simpler GL theory.

### B. Surface dipole

The second kind of charges determining the electrostatic potential is a surface dipole due to which the potential has a finite step. A spatially resolved profile of this

step is not known. It is expected that the dipole is located near the surface inside the superconductor. In analogy with the space profile of the superconducting gap, one can speculate that the width of the dipole is similar to the BCS coherence length  $\xi_0$ . The present treatment is limited to temperatures close to  $T_c$ , where  $\xi_0 \ll \xi$ . Accordingly, we assume the width of the surface dipole to be infinitesimal.

So far, the role of the surface dipole in superconductors is not fully clarified. There is an important experimental experience with the electrostatic potential above the surface in the Meissner state, however. Precise measurements of the electrostatic potential made by Morris and Brown<sup>17</sup> with the help of the capacitive Kelvin method have shown a surprising result – all contributions of the pairing forces<sup>9,10</sup> are canceled by the surface dipole. The experiment of Morris and Brown thus indicates that the surface dipole has to be taken into account.

Based on the assumption that the surface dipole results from the surface depression of the BCS gap, we have derived in Ref. 6 the local value of the dipole as a function of the GL wave function at the surface. The internal electrostatic potential and the potential step due to the surface dipole add. The resulting observable surface potential

$$e\phi_0 = -\frac{f_{el}}{n} \quad (1)$$

is given by the free energy per electron.<sup>6</sup> Here  $n$  is the total density of pairable electrons (the total density) and  $f_{el}$  is the density of the electronic part of the free energy.

The surface potential (1) follows from general thermodynamic assumptions and it can be implemented within different approximations of the free energy, compare Ref. 6 with Ref. 18. In our treatment the free energy is evaluated from the GL theory.

### C. Surface charge

Finally, there is the surface charge distributed on the scale of the Thomas-Fermi screening length,  $\lambda_{TF}$ , from the surface. Since  $\lambda_{TF}$  is much shorter than the GL coherence length  $\xi$ , the BCS coherence length  $\xi_0$ , and the London penetration depth  $\lambda$ , we use the limit  $\lambda_{TF} \rightarrow 0$  and treat the surface charge as an ideal two-dimensional surface charge. The surface charge represents the utmost layer of the superconductor.

The surface charge simplifies the construction of the electrostatic potential inside and outside of the superconductor.<sup>1</sup> Neglecting contributions of the order of  $\lambda_{TF}^2/\xi^2$ , one can simply evaluate the potential at the inner side of the surface,  $\phi(0_-)$ , and match it with the potential outside,  $\phi(0_+) = \phi(0_-)$ . The potential outside decays far from the surface to its mean value,  $\phi(z) \rightarrow \langle \phi \rangle$  for  $z \rightarrow \infty$ . Due to this asymptotic condition, the potential is fully specified by its value at the surface. In

our case the potential at the surface includes the surface dipole,  $\phi(0_+) = \phi(0_-) = \phi_0$ , where  $\phi_0$  is given by formula (1).

The matching of the inner and outer potentials is simple in the two-dimensional Fourier representation,

$$\phi(\mathbf{K}) = \frac{2}{\Omega} \int_{\Omega} d\mathbf{r} \phi_0(\mathbf{r}) \cos(\mathbf{K}\mathbf{r}), \quad (2)$$

where  $\mathbf{r} \equiv (x, y)$  and  $\mathbf{K}$  are discrete momenta that have to be selected according to the structure of the Abrikosov vortex lattice. The area  $\Omega$  of the elementary cell is given by the mean magnetic field  $B$  and the elementary flux,  $\Phi_0 = B\Omega$ . One obtains the potential at any distance  $z > 0$  from the surface,

$$\phi(\mathbf{r}, z) = \langle \phi \rangle + \sum_{\mathbf{K} \neq 0} \phi(\mathbf{K}) e^{-|\mathbf{K}|z} \cos(\mathbf{K}\mathbf{r}), \quad (3)$$

from the Fourier components (2) and the mean value  $\langle \phi \rangle = \frac{1}{\Omega} \int d\mathbf{r} \phi_0(\mathbf{r})$ . It is easy to check that the potential (3) satisfies the Poisson equation.

The potential or its gradient at a finite distance will naturally be necessary for interpretations of future measurements. On the other hand, we feel that this technical step does not bring any new insight to the problem. In our discussion we will focus on the surface value  $\phi_0(\mathbf{r}) = \phi(\mathbf{r}, 0)$ .

### III. SURFACE POTENTIAL WITHIN THE GINZBURG-LANDAU THEORY

With respect to electrostatic phenomena it is advantageous to introduce the GL theory in the formulation proposed by Bardeen.<sup>19,20</sup> The free energy

$$f_{\text{el}} = \frac{1}{2} \gamma T^2 + \frac{1}{2m^*} \bar{\psi} (-i\hbar \nabla - e^* \mathbf{A})^2 \psi - \varepsilon_{\text{con}} \frac{2|\psi|^2}{n} - \frac{1}{2} \gamma T^2 \sqrt{1 - \frac{2|\psi|^2}{n}} \quad (4)$$

is composed of three terms: the free energy of Gorter and Casimir (last two terms), the kinetic energy in the quantum form (second term), and the subtracted free energy of the normal state (first term). Here,  $\gamma$  is the linear coefficient of the specific heat. The condensation energy determines the critical temperature as  $\varepsilon_{\text{con}} = \frac{1}{4} \gamma T_c^2$ .

For temperatures close to  $T_c$  the superconducting fraction is small,  $\frac{2|\psi|^2}{n} \ll 1$ . Expanding the square root in this small value one arrives at the GL free energy

$$f_{\text{el}} = \frac{1}{2m^*} \bar{\psi} (-i\hbar \nabla - e^* \mathbf{A})^2 \psi + \alpha |\psi|^2 + \frac{1}{2} \beta |\psi|^4. \quad (5)$$

Note that the kinetic energy is not in the form proposed by Ginzburg and Landau<sup>21</sup>. In particular, it becomes negative at the vortex core. The volume integral over this kinetic energy differs from the GL form by a surface

contribution which is identically zero if the GL boundary condition is satisfied, see the discussion in Ref. 22.

From the limit  $\frac{2|\psi|^2}{n} \rightarrow 0$  one obtains the GL parameters  $\alpha = -\frac{1}{2n} \gamma (T_c^2 - T^2)$  and  $\beta = \frac{1}{2n^2} \gamma T^2$ . Below we compare the surface potential with the bulk potential. The bulk potential includes pairing forces proportional to density derivatives  $\frac{\partial \alpha}{\partial n}$  and  $\frac{\partial \beta}{\partial n}$ . The temperature dependence is essential in this point as  $\frac{\partial T_c}{\partial n} \neq 0$ . After we have evaluated derivatives, we can use the usual limiting parameters of the GL theory,  $\alpha = -\frac{1}{n} \gamma T_c (T_c - T)$  and  $\beta = \frac{1}{2n^2} \gamma T_c^2$ .

To complete the description of the GL free energy we recall that the charge of the Cooper pair equals twice the electron charge,  $e^* = 2e$ . The mass  $m^* = 2m$  depends on impurities and has to be fitted, e.g., from the GL coherence length using  $\xi^2 m^* \gamma (T_c^2 - T^2) = n \hbar^2$ . For Niobium we use  $T_c = 9.5$  K and  $\gamma = 719$  J/(m<sup>3</sup>K<sup>2</sup>) giving  $\varepsilon_{\text{con}} = 1.6 \cdot 10^4$  J/m<sup>3</sup>. The electron density is  $n = 2.2 \cdot 10^{28}$ /m<sup>3</sup>, so that the condensation energy per particle is  $\varepsilon_{\text{con}}/n = 4.59$   $\mu$ eV. For pure Niobium the effective mass is  $m = 1.2 m_e$  and the GL parameter is  $\kappa = 0.78$ .

#### A. The surface potential

To proceed we have to derive the GL equation for the GL wave function  $\psi$ . For the assumed thin layer, induced currents are proportional to the layer width  $L$  and they are negligible in the limit  $L \ll \lambda$ . The vector potential  $\mathbf{A}$  thus has the same value as in the absence of the superconducting layer and  $\mathbf{B}$  is practically constant in thin layers<sup>23</sup>.

From the minimum of the free energy we arrive at the GL equation

$$\frac{(-i\hbar \nabla - e^* \mathbf{A})^2}{2m^*} \psi = -\alpha \psi - \beta |\psi|^2 \psi. \quad (6)$$

This equation is solved numerically with the help of the iteration procedure described in Ref. 24.

Before we enter a discussion of numerical results presented in the next section, it is useful to express the surface potential as a function of the amplitude of the GL wave function. To this end we multiply (6) by  $\bar{\psi}$  which yields  $\frac{1}{2m^*} \bar{\psi} (-i\hbar \nabla - e^* \mathbf{A})^2 \psi = -\alpha |\psi|^2 - \beta |\psi|^4$ . If we substitute this relation into the free energy (5), we find that the free energy is the negative value of the quartic term  $f_{\text{el}} = -\frac{1}{2} \beta |\psi|^4$ . The surface potential (1) thus attains the simple form

$$e\phi_0 = \frac{1}{2n} \beta |\psi|^4. \quad (7)$$

At this point we can stress the first effect of the surface dipole. According to (7), the electrostatic potential is proportional to  $|\psi|^4$ . In contrast, the internal potential

used by Blatter *et al.*

$$e\phi_{\text{Bl}} = \frac{\gamma T_c}{n} \frac{\partial T_c}{\partial n} |\psi|^2 \quad (8)$$

is proportional to  $|\psi|^2$ . The different order of the amplitude does not ruin the basic idea of the proposed experiment – the electrostatic potential at the surface can be used to monitor the GL wave function.

### B. Upper estimate of the amplitude

It is possible to establish an upper estimate of the amplitude of the electrostatic potential. The minimum of the potential (7) is at a vortex center, where  $e\phi_0 \rightarrow 0$  since  $|\psi|^2 \rightarrow 0$ .

The potential  $e\phi_0$  reaches its maximum somewhere between vortices. The magnetic field in the Abrikosov vortex lattice suppresses the amplitude of the GL wave function compared to its value  $\psi_\infty^2 = -\frac{\alpha}{\beta}$  in the non-magnetic state. Therefore from  $|\psi|^2 \leq \psi_\infty^2$  one obtains an upper estimate of the maximum as

$$e\phi_0 \leq \frac{1}{2n} \frac{\alpha^2}{\beta} = \frac{\varepsilon_{\text{con}}}{n} 4(1-t)^2. \quad (9)$$

Here we have used  $\alpha = (-4\varepsilon_{\text{con}}/n)(1-t)$ , where  $t = T/T_c$ , to highlight that close to the critical temperature the amplitude of the potential vanishes as  $(1-t)^2$ .

To illustrate how the surface dipole changes the surface potential we compare the full potential (7) with the internal potential (8). For the amplitude of the internal potential (8) one has the upper estimate

$$e\phi_{\text{Bl}} \leq -\frac{\gamma T_c}{n} \frac{\partial T_c}{\partial n} \frac{\alpha}{\beta} = \frac{\varepsilon_{\text{con}}}{n} \frac{\partial \ln T_c}{\partial \ln n} 8(1-t). \quad (10)$$

For Niobium one finds from the McMillan formula the value  $\frac{1}{2}\gamma T_c \frac{\partial T_c}{\partial n} = 6.78 \mu\text{eV}$ , see Ref. 11. This corresponds to  $\frac{\partial \ln T_c}{\partial \ln n} = 0.74$ . Numerical factors of the surface potential (9) and the internal potential (10) are thus quite comparable. What makes the difference is the temperature dependence.

### C. Lower temperatures

The above upper estimate of the potential amplitude is based on the zero free energy at the vortex center and the finite free energy in the non-magnetic state. These values can be easily estimated also at temperatures far from  $T_c$ . Indeed, as long as the free energy is adjusted to vanish in the normal state, it has to be zero at the vortex center, where the superconducting condensate vanishes. The free energy in the non-magnetic state can be taken from the thermodynamic measurements in the form  $f_{\text{el}} =$

$-\varepsilon_{\text{con}}(1-t^2)^2$ . Accordingly, the upper estimate of the amplitude of the potential is

$$e\phi_0 \leq \frac{\varepsilon_{\text{con}}}{n} (1-t^2)^2. \quad (11)$$

This estimate applies to any temperature. Of course, it approaches (9) for  $t \rightarrow 1$ .

Similarly we can use the relation between the GL wave function and the superconducting density  $2|\psi|^2 = n_s$  together with the phenomenological law  $n_s = n(1-t^4)$  to obtain the estimate of the internal potential

$$e\phi_{\text{Bl}} \leq \frac{\varepsilon_{\text{con}}}{n} \frac{\partial \ln T_c}{\partial \ln n} 2(1-t^4). \quad (12)$$

For  $t \rightarrow 1$  this estimate goes to (10).

One can see that for low temperatures,  $t \ll 1$ , estimates (11) and (12) yield comparable amplitudes of the potential. This indicates that at low temperatures the surface dipole is less effective in reducing the surface potential.

## IV. NUMERICAL RESULTS FOR NIOBIUM

Now we discuss the electrostatic potential with the help of numerical results. To be specific, we use material parameters of Niobium.

Figure 1 displays the GL wave function  $\omega \equiv |\psi|^2/\psi_\infty^2$ , where  $\psi_\infty$  is the GL wave function in the absence of the magnetic field,  $2\psi_\infty^2 = n(1-t^4)$ . The profile of  $\omega$  is compared with the surface electrostatic potential  $\phi_0$  according to equation (7) near the critical temperature,  $T = 0.95 T_c$ .

In the first row we show the result for Niobium with  $\kappa = 1.5$ . The low magnetic field  $B = 0.06 B_{c2}$  already falls into the limit of isolated vortices, because vortex cores are well separated and the superconducting fraction between them reaches its non-magnetic value with less than 1% difference. The amplitude of the electrostatic field is thus well described by the estimate (11).

Compared to the superconducting fraction, the electrostatic potential is much flatter in the center of the vortex. This feature directly follows from formula (7). At the vortex center,  $x^2 + y^2 = r^2 \rightarrow 0$ , the superconducting fraction quadratically vanishes with  $r$ ,  $\omega \propto r^2$ . According to (7) the potential vanishes there with the fourth order of  $r$ ,  $\phi_0 \propto r^4$ . We believe that this will be possible to be observed in future measurements.

The second row in figure 1 with  $\kappa = 0.78$  corresponds to pure Niobium. We choose the magnetic field close to the upper critical field  $B = 0.7818 B_{c2}$ , when the superconducting fraction is suppressed to less than 1/3 of its non-magnetic value. In this regime the GL wave function is well approximated by the asymptotic solution due to Abrikosov.<sup>25</sup>

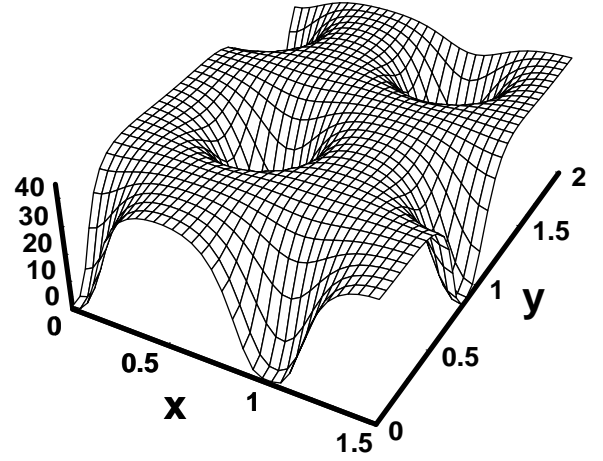
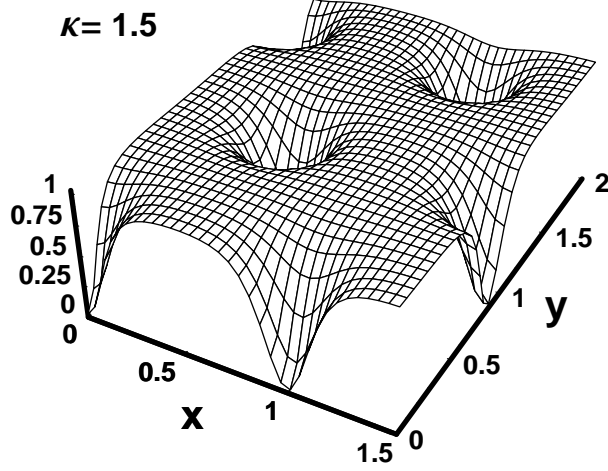
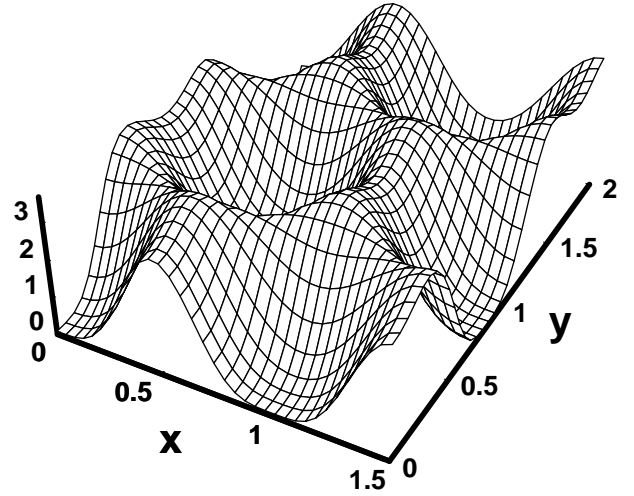
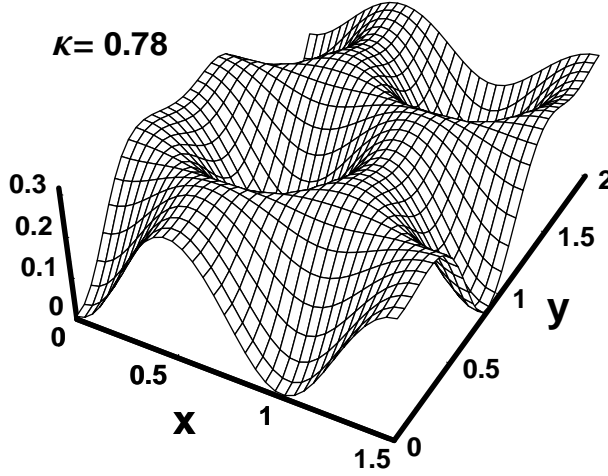
**B/B<sub>c2</sub>(T)= 0.06** **$\omega$**  **$\phi$  [nV]** **$\kappa= 1.5$** **B/B<sub>c2</sub>(T)= 0.78** **$\kappa= 0.78$** 

FIG. 1. The relative superconducting fraction  $\omega = |\psi|^2/\psi_\infty^2$  (left column) and the electrostatic potential  $\phi$  (right column) at the surface of the superconductor with the Abrikosov vortex lattice. The distances are normalized to the vortex separation. The temperature  $T = 0.95 T_c$  is used for both cases, the GL parameter  $\kappa$  and the magnetic field are specified for each row. Material parameters are of Niobium.

### A. Estimate from the Abrikosov solution

For  $B$  close to  $B_{c2}$ , the amplitude of the GL wave function undergoes rapid changes while its shape remains nearly unchanged. As in Fig. 1 we express the superconducting fraction,  $2|\psi|^2/n$ , in terms of its non-magnetic value,  $2|\psi_\infty|^2/n = 1 - t^4$  as the relative superconducting fraction  $\omega = |\psi|^2/|\psi_\infty|^2$ .

For the fixed shape of the GL wave function, the mean  $\langle\omega\rangle = \frac{1}{\Omega} \int d\mathbf{r} \omega$  and its fluctuation  $\langle\omega^2\rangle = \frac{1}{\Omega} \int d\mathbf{r} \omega^2$  are proportional as  $\langle\omega^2\rangle = \beta_A \langle\omega\rangle^2$ , where the Abrikosov coefficient for the triangular lattice is  $\beta_A = 1.16$ . Taking  $1 - b$  with  $b = B/B_{c2}$  as a small perturbation, one finds that the free energy (5) has the minimum when  $\langle\omega^2\rangle = \langle\omega\rangle(1 - b)$ . The mean and the fluctuations thus read\*

$$\langle\omega\rangle = \frac{1}{\beta_A} (1 - b), \quad \langle\omega^2\rangle = \frac{1}{\beta_A} (1 - b)^2. \quad (13)$$

With the help of the mean values (13) we can express the mean values of the electrostatic potentials. The surface potential (7) with the surface dipole included has the mean value

$$\langle e\phi_0 \rangle = \frac{\varepsilon_{\text{con}}}{n} (1 - t^2)^2 \frac{1}{\beta_A} (1 - b)^2. \quad (14)$$

If we extend the estimate by Blatter *et al.* to magnetic fields close to the critical field, we find that it has the mean value

$$\langle e\phi_{\text{Bl}} \rangle = \frac{\varepsilon_{\text{con}}}{n} \frac{\partial \ln T_c}{\partial \ln n} 2(1 - t^4) \frac{1}{\beta_A} (1 - b). \quad (15)$$

Comparing (14) with (15) one can see that due to the surface dipole, the electrostatic potential vanishes close to the upper critical field as  $(1 - b)^2$ , rather than  $1 - b$  without the dipole. We expect that this dependence on the magnetic field might be one of experimentally well accessible tests of the presence of the surface dipole.

### B. Effect of the surface dipole

As already mentioned the surface dipole is responsible for the flat region of the potential at the center of the vortex. In this section we discuss the role of the surface dipole in more detail.

In Fig. 2 we compare the present theory yielding formula (7) with three approximations. First, if one neglects the surface dipole, the surface potential becomes equal to the internal potential<sup>11</sup>

---

\*For details of the derivation see Ref. 25. In the limit of the thin layer the term  $\langle\omega^2\rangle/2\kappa^2$  disappears as it follows from the induced magnetic field.

$$e\phi = -\frac{1}{2m^*n} \bar{\psi} (-i\hbar\nabla - e^*\mathbf{A})^2 \psi + \frac{\partial\varepsilon_{\text{con}}}{\partial n} \frac{2|\psi|^2}{n} - \frac{T^2}{2} \frac{\partial\gamma}{\partial n} \left( \frac{|\psi|^2}{n} + \frac{|\psi|^4}{2n^2} \right). \quad (16)$$

The material parameters for Niobium  $\frac{\partial\varepsilon_{\text{con}}}{\partial n} = 8.71 \mu\text{eV}$  and  $\frac{1}{2} \frac{\partial\gamma}{\partial n} T_c^2 = 3.85 \mu\text{eV}$ , are derived in Ref. 11.

Second, the surface dipole results from the pairing forces. As long as one does not account for the surface dipole, perhaps it is better to neglect also other pairing forces. In this approximation the surface potential equals the first term of equation (16) which covers the inertial and Lorentz forces.

Third, following Blatter *et al.* we take a single vortex located at  $x, y = 0$ . Its GL wave function is modeled by the Clem ansatz<sup>26</sup>  $\omega \approx 1 - \xi_v^2/(x^2 + y^2 + \xi_v^2)$ . The vortex radius  $\xi_v$  found from the minimum of the free energy is given by  $\xi_v = \xi\sqrt{2}\sqrt{1 - K_0^2(\xi_v/\lambda)/K_1^2(\xi_v/\lambda)}$ , where  $K_0$  and  $K_1$  are modified Bessel functions. According to the approximation of Khomskii and Kusmartsev<sup>3</sup> adopted by Blatter *et al.*, we take only the second term of equation (16) with  $\frac{\partial\varepsilon_{\text{con}}}{\partial n} \approx \frac{1}{2}\gamma T_c \frac{\partial T_c}{\partial n} = 6.78 \mu\text{eV}$ .

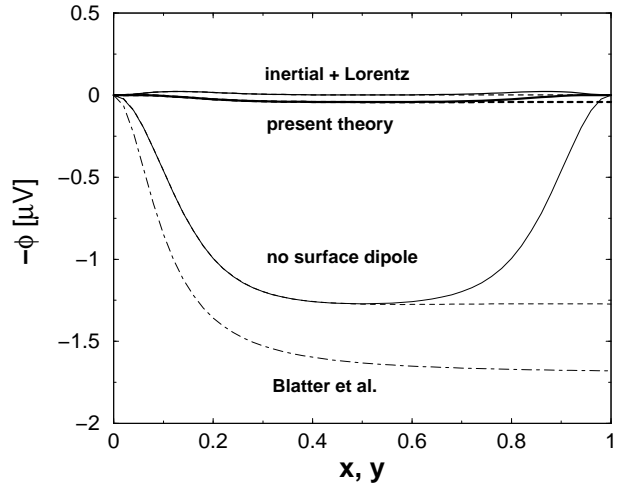


FIG. 2. Various approximations of the electrostatic potential at the surface. The parameters  $T = 0.95 T_c$ ,  $\kappa = 1.5$  and  $B = 0.7818 B_{c2}$  correspond to the upper right plot in Fig. 1. The symmetric lines (solid) are cuts along the  $x$  axis, the non-symmetric lines (dashed) are cuts along the  $y$  axis in Fig. 1. The line ‘present theory’ is given by eq. (7), the line ‘no surface dipole’ by eq. (16), the line ‘inertial + Lorentz’ corresponds to the first term of eq. (16), and the line ‘Blatter *et al.*’ is according to Ref. 1.

The potentials plotted in Fig. 2 can be sorted into two groups. The internal potential (16) and Blatter’s result are very similar except for some minor differences following from the Clem model and the neglect of  $\frac{\partial\gamma}{\partial n}$ . The potential (7) with the surface dipole included, and the approximation by inertial and Lorentz forces are much smaller than the potentials from the first group.

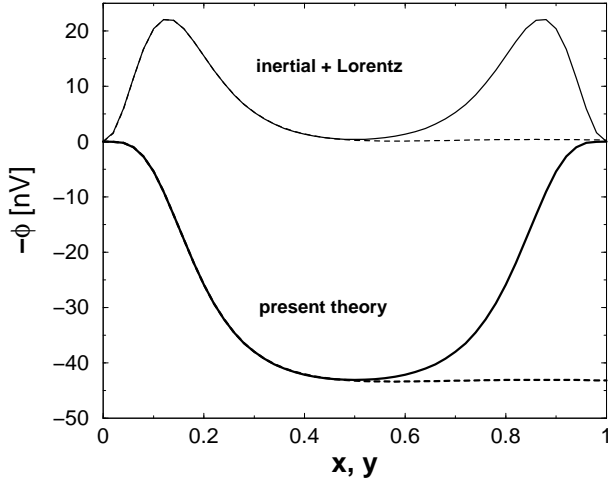


FIG. 3. Detail of Fig. 2.

To compare our potential (7) with the approximation by inertial and Lorentz forces, we have expanded the scale in Fig. 3. The numerical result clearly shows that the approximation by inertial and Lorentz forces has a very different profile. Briefly, above the Abrikosov vortex lattice the surface dipole cancels the major part of the contribution of pairing forces. On the other hand, it is not possible to avoid the full calculation and to replace the action of the surface dipole by simply omitting the pairing forces.

Figure 4 shows the different potentials for  $\kappa = 0.78$  corresponding to pure Niobium of the lower row in Fig. 1. Most of the features are identical to the situation of larger  $\kappa$  in the upper row in Fig 1 and in Fig. 2. But, in the internal potential (16) the GL wave function is now suppressed by the magnetic field compared to Blatter's approach. Indeed, the Clem approximation is derived for the limit of low magnetic fields and thus it does not cover the suppression.

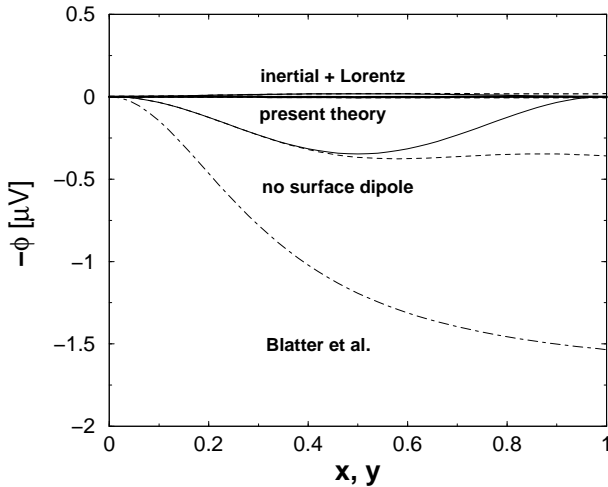


FIG. 4. The same as Fig. 2 but with parameters of the lower row in Fig. 1, i.e.,  $T = 0.95 T_c$ ,  $\kappa = 0.78$  and  $B = 0.78 B_{c2}$ .

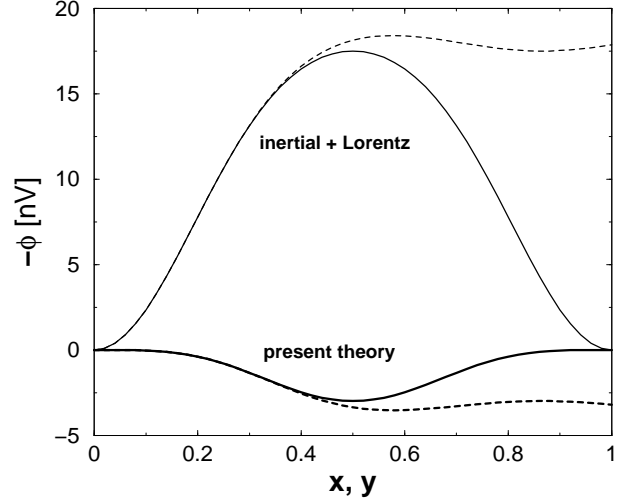


FIG. 5. Detail of Fig. 4.

The detail presented in Fig. 5 demonstrates that the full theory and the approximation by inertial and Lorentz forces result in very different profiles of the electrostatic potential. One can see that the neglect of pairing forces leads to the potential of much larger amplitude and the wrong sign.

## V. SUMMARY

We have evaluated the electrostatic potential above the surface of a thin superconducting layer with the Abrikosov vortex lattice. It has been shown that the surface dipole strongly modifies the magnitude of this potential, in particular when the GL wave function has a small magnitude. This is due to the relation  $\phi_0 \propto |\psi|^4$ , see (7), while without the dipole one finds  $\phi_{BI} \propto |\psi|^2$ .

According to various mechanisms to suppress the GL wave function, we can outline possible cases for which the presented theory can be tested. At the vortex core  $|\psi|^2 \propto r^2$  so that  $\phi_0 \propto r^4$  while  $\phi_{BI} \propto r^2$ . At temperatures close to the critical temperature,  $t \rightarrow 1$ ,  $|\psi|^2 \propto 1 - t$ , therefore  $\phi_0 \propto (1 - t)^2$  while  $\phi_{BI} \propto 1 - t$ . Finally, at magnetic fields close to the upper critical field,  $b \rightarrow 1$ ,  $|\psi|^2 \propto 1 - b$  so that  $\phi_0 \propto (1 - b)^2$  while  $\phi_{BI} \propto 1 - b$ . Of course, there is a rich area of experimental realizations with mesoscopic superconducting devices.

We would like to mention limitations of our approach. First, the formula for the surface potential has been derived only for the magnetic field parallel to the surface. According to its interpretation in terms of the pairing energy we believe that it also applies for the perpendicular field, nevertheless, its validity should be tested. Second, the local approximation of the surface dipole requires the BCS coherence length  $\xi_0$  to be much smaller than the GL coherence length  $\xi$ . This is satisfied at temperatures close to the critical temperature, while one can expect sharper spatial profiles at lower temperatures. For this region of

lower temperature, however, our results have to be taken only qualitatively.

## ACKNOWLEDGMENTS

We would like to thank H. Shimada who stimulated our interest in this problem. This work was supported by MŠMT program Kontakt ME601 and GAČR 202/03/0410 and 202/04/0585, GAAV A1010312 grants and DAAD project D/03/44436. The European ESF program AQDJJ is also acknowledged.

- 
- <sup>1</sup> G. Blatter, M. Feigel'man, V. Geshkenbein, A. Larkin and A. van Otterlo, Phys. Rev. Lett. **77**, 566 (1996).  
<sup>2</sup> K. M. Hong, Phys. Rev. B. **12**, 1766 (1975).  
<sup>3</sup> D. I. Khomskii and F. V. Kusmartsev, Phys. Rev. B **46**, 14245 (1992).  
<sup>4</sup> D. I. Khomskii and A. Freimuth, Phys. Rev. Lett. **75**, 1384 (1995).  
<sup>5</sup> H. Shimada, private communication.  
<sup>6</sup> P. Lipavský, K. Morawetz, J. Koláček, J. J. Mareš, E. H. Brandt and M. Schreiber, Phys. Rev. B **70**, 104518 (2004).  
<sup>7</sup> M. A. R. LeBlanc, Supercond. Sci. Technol. **10**, 929 (1997).  
<sup>8</sup> J. Koláček, P. Lipavský and E. H. Brandt, Phys. Rev. Lett. **86**, 312 (2001).  
<sup>9</sup> C. J. Adkins and J. R. Waldram, Phys. Rev. Lett. **21**, 76 (1968).  
<sup>10</sup> G. Rickayzen, J. Phys. C **2**, 1334 (1969).  
<sup>11</sup> P. Lipavský, J. Koláček, K. Morawetz and E. H. Brandt, Phys. Rev. B **65**, 144511 (2002).  
<sup>12</sup> T. Koyama, J. Phys. Soc. Jpn. **70**, 2102 (2001).  
<sup>13</sup> M. Machida and T. Koyama, Physica C **378**, 443 (2002).  
<sup>14</sup> M. Machida and T. Koyama, Physica C **388**, 659 (2003).  
<sup>15</sup> M. Machida and T. Koyama, Phys. Rev. Lett. **90**, 077003 (2003).  
<sup>16</sup> X.Y. Jin and Z.Z. Gan, Eur. Phys. J. B **37**, 489 (2004).  
<sup>17</sup> T. D. Morris and J. B. Brown, Physica **55**, 760 (1971).  
<sup>18</sup> P. Lipavský, J. Koláček, J. J. Mareš and K. Morawetz, Phys. Rev. B **65**, 012507 (2001).  
<sup>19</sup> J. Bardeen, Phys. Rev. **94**, 554 (1954).  
<sup>20</sup> J. Bardeen, *Theory of Superconductivity* in Handbuch der Physik, Bd. XV, 274 (Springer Berlin, 1956).  
<sup>21</sup> W. L. Ginsburg and L. D. Landau, Zh. Eksp. Teor. Fiz. **20**, 1064 (1950).  
<sup>22</sup> J. R. Waldram, *Superconductivity of Metals and Cuprates*, Chap. IV.3 (IOP Publishing Ltd, London, 1996).  
<sup>23</sup> E. H. Brandt, Phys. Rev. B **68**, 054506 (2003).  
<sup>24</sup> E. H. Brandt, Phys. Rev. Lett. **78**, 2208 (1997).  
<sup>25</sup> P. G. de Gennes, *Superconductivity of Metals and Alloys*, Chap. VI.7. (Benjamin, New York, 1966).  
<sup>26</sup> J. R. Clem, J. Low Temp. Phys. **18**, 427 (1975).